

Soft robotic tactile perception of softer objects based on learning of spatiotemporal pressure patterns

Tetsushi Nonaka¹, Arsen Abdulali², Chapa Sirithunge², Kieran Gilday² and Fumiya Iida²

Abstract—The softness perception of objects with lower stiffness than that of robotic skin is challenging, as the proportion of the deformation of skin to that of an object’s surface is unknown. This makes it difficult to derive the indentation depth typically used for stiffness estimation. To overcome this challenge, we implemented human-inspired softness sensing in a soft anthropomorphic finger based on tactile information alone without using the information about indentation depth or displacement. In the experiments where LSTM networks were trained to discriminate viscoelastic soft objects, we demonstrated that the sensorized robotic finger using tactile information from barometric sensors embedded in its soft skin could successfully learn to discriminate soft objects. By dissociating the relative contribution of the dynamic pattern of pressure distribution and that of local pressure, we further investigated how differences in available tactile information could impact the ability to distinguish the softness of viscoelastic objects. The results demonstrated that the pressure distribution and its change on the soft contact area of the robotic finger provided information to discriminate the softness of viscoelastic objects and that the tactile information about softness was spatiotemporal in nature. The results further implied that nonlinear local dynamics such as hysteresis in local pressure changes can provide additional information about the viscoelasticity of touched objects.

Index Terms—Softness perception, tactile sensing, haptics, touch, viscoelasticity, compliance

I. INTRODUCTION

Delicate handling of natural objects, e.g., picking a ripe raspberry and palpating soft tissues, is one of the possible advantages of soft robots over traditional rigid counterparts [1]–[3]. However, the softness perception of objects with comparable or lower stiffness than that of a robotic skin becomes challenging, as the information about indentation depth, typically used for stiffness estimation, is often unavailable. Tracking the deformation of an object’s surface occluded by contacting part of a robot is very difficult. Positions of robotic joints are also impractical [4], [5], as the proportion of the finger skin deformation to the one of an object’s surface is unknown. Therefore, softness discrimination remains among the unresolved challenges in soft robotics [6]–[8]. The goal of the present study is two-fold. First, we aim to implement softness sensing in a soft robotic finger based on tactile information (referring to the sense of pressure distribution and its change in the neighborhood of the contact area) without using the

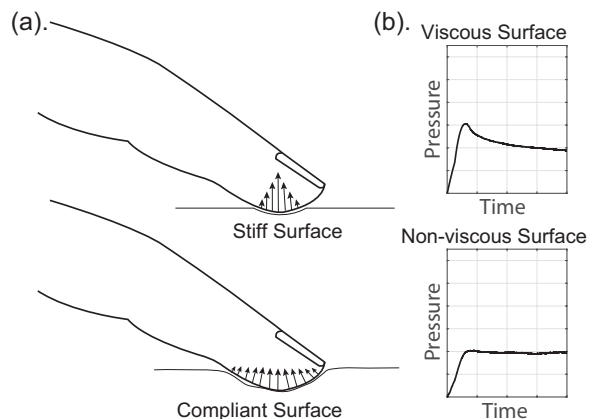


Fig. 1. Examples of tactile information available in discriminating an object’s softness. (a) Spatial information: The shape and size of the contact area, and the pattern of force distribution over this area changes according to the compliance of the touched object. (b) Temporal information: Even when the finger remains still in contact with objects, the magnitude of pressure changes depending on the viscosity the contacted objects. That is, there is a phase difference between changes of pressure that arise from the indentation of a finger and those that arise from the viscosity of material.

information about indentation depth or displacement of the finger, by taking advantages of complex dynamics at the skin-object interface upon physical contact between soft skin and objects. Second, we aim to investigate how differences in available tactile information impact the ability to distinguish the softness of viscoelastic materials, dissociating the relative contribution from the spatial distribution of pressure and its change, and local pressure dynamics, laying the ground for implementing sensing of very soft objects in soft robotic systems.

In humans, the acuity of tactile perception of soft objects is known to be a function of several interrelated factors [9]–[12]. Previous experiments involving passive touch, in which compliant objects were applied to the fingerpad in a passive manner, have shown that tactile information alone was sufficient to discriminate the compliance of the touched objects with deformable surfaces, even if the velocities and forces of objects application were randomized and unknown [13]. Physical contact with compliant objects such as when pressing it with a fingerpad introduces complex dynamic interaction at the skin-object interface that depends on the mechanical properties of both the fingerpad and the objects. In particular, for objects with deformable surfaces, how the area of contact spreads and how the pressure is distributed over the contact area heavily depend on the compliance of the touched objects [14]–[16]. Consequently, the contact area, its shape (eccentricity), spatial pressure distribution

*This work was not supported by any organization

¹ Graduate School of Human Development and Environment, Kobe University 657-8501, Japan. tetsushi@people.kobe-u.ac.jp

² Department of Engineering, University of Cambridge, Cambridge CB2 1PZ, UK. {aa2335, csh66, kg398, fi224}@cam.ac.uk

within the contact area, and their temporal variation would be distinct for objects with different degrees of compliance (Fig. 1a), which provide important information for discriminating softness [14], [15], [17]. Put differently, by taking advantage of complex mechanical interaction arising from the passive dynamics of the finger and soft objects, humans are able to obtain information about the softness of objects, without relying on the information about the displacements of fingers and limbs. Subsequent studies have further shown that individuals with softer skin exhibit larger gross contact areas and larger surface deformation upon contact with objects, resulting in higher perceptual acuity in the discrimination of compliance of the material being touched [18]. These results suggest that spatial patterns of dynamic cutaneous deformation of relatively large contact areas at the fingertip as opposed to local changes of pressure itself provide important perceptual information about softness. Yet, the extent of the impact of different kinds of sensory information on tactile acuity in discriminating softness still remains unclear [19].

There is another important but often neglected issue regarding the perception of softness. Deformable soft materials which we interact with in our daily lives exhibit different mechanical behaviors in different dimensions such as viscosity, not only in a single dimension of compliance [20], [21]. In particular, viscoelastic behavior is commonly observed in biological materials, and the judgments about viscoelastic properties of soft materials can be of critical importance in certain settings like clinical practices [22]. The mechanical behavior of soft materials lies in a range that is between purely elastic and purely viscous. History- and frequency-dependent behavior of viscoelastic materials result in a complex time-dependent response (Fig. 1b), which could potentially provide important information about the properties of soft objects [21]. Yet, while the information underlying the perception of compliance has been addressed in a number of studies, the perceptual information underlying the softness in the dimension of viscosity has rarely been studied in biological and artificial systems alike [20], [21].

Inspired by human softness perception, herein, we aim to implement softness sensing in a soft robotic finger based on tactile information, and to further investigate how differences in available tactile information impact the ability to distinguish the softness of viscoelastic materials. The results of previous human experiments led us to the following set of interrelated hypotheses. First, we hypothesized that a soft robotic finger, which is sensitive to the distribution of pressure and its dynamics on the deformable contact area, could discriminate the compliance of objects without relying on kinesthetic information. We tested this hypothesis by evaluating the performance of recurrent neural networks that are trained to discriminate fourteen very soft objects that vary in compliance and viscosity, using the data from the six sensors connected to the air chambers embedded in the soft skin of the finger. Second, we hypothesized that the tactile information that the soft finger uses to discriminate compliance is spatiotemporal

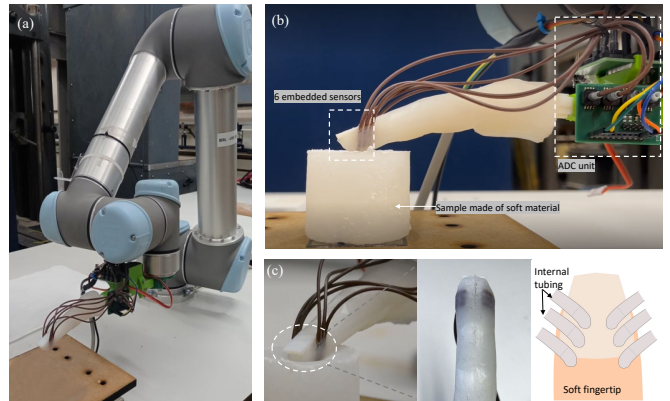


Fig. 2. (a) The soft finger attached to a UR5 robotic manipulator (b) The anthropomorphic soft finger interacting with a soft sample on the ground-truth FSR sensor for learning (c) The fingertips with embedded pressure chambers for internal tubing.

in nature and that the discrimination performance deteriorates when information about the spatial distribution of pressure is not available. To test this hypothesis, we compared the discrimination performance by neural networks between the condition where only local pressure information (i.e., the data from one sensor) is available and the condition where information about the distribution of pressure is available. Third, we hypothesized that the kind of tactile information available for discriminating soft objects would be different in viscous objects and non-viscous objects and that the temporal pattern of pressure in itself would provide important information in discriminating viscous soft objects. The contribution of the present study lies in presenting the data that clearly delineate the kind of tactile information about softness that can be potentially used in soft robotic fingers.

II. METHODS

The work investigates whether a soft robotic finger could successfully learn to discriminate a set of objects with different softness without using the information about displacement of the finger. We prepared two sets of seven soft objects (low viscosity set and high viscosity set) with different degrees of compliance, yielding fourteen objects in total. A soft robotic finger mounted on a robotic manipulator was indented into each of the fourteen soft objects 600 times, where the displacement and velocity of indentation were randomized. Using the sensor data from the robotic finger, whose magnitude was normalized between 0 - 1 to eliminate the baseline difference of pressure, the LSTM recurrent neural network was trained for multi-class discrimination of the fourteen soft objects. The comparison of discrimination performances of the LSTM network trained with different conditions is expected to reveal how the acuity of discrimination is attributed to distinct tactile information available.

A. Sensorized Soft Robotic Finger

The anthropomorphic finger, as shown in Fig. 2 (a), consists of a 3D printed skeleton with silicone-casted artificial skin (Ecoflex 00-10, Smooth-On Inc.). The characteristic of the silicone layer resembles the natural dynamics of the human flesh, which in turn, deforms and dynamically changes the pressure distribution over the contact area depending on the property of the to-be-contacted object and the kind of contact with the object in the environment [23]. To measure the contact forces of the contact, six air chambers were cast at the tip of the anthropomorphic finger and connected to NXP MPXH6300AC6U pressure sensors via elastic hoses [24]. The air chamber would affect the stiffness of the skin where the finger is pressed, but would not affect the overall stiffness as the deformation is localized around each joint. Each air chamber was less than 10 mm^3 in volume, and its internal pressure has a negligible effect on the stiffness of the entire finger.

B. Soft Objects

Objects with varied softness were created by mixing silicone rubber EcoFlex 00-10, with Slacker, and Silicon Thinner (Smooth-On, Inc) as softening agents. These are pourable silicone rubbers that cure at room temperature under the addition of a medium. Increasing the amount of Slacker and Silicon Thinner both decreases stiffness, but in a different manner. Increasing the amount of Slacker increases viscosity, whereas increasing the amount of Silicon Thinner decreases viscosity [25].

Fourteen different mixing ratios were used, encompassing the range of compliance and viscosity. First, by using Slacker as a softening agent, materials with high viscosity with intermediate compliance were attained as following ratios (EcoFlex 00-10 part A + B, and Slacker, respectively): 1:0.8 (S80), 1:1.0 (S100), 1:1.2 (S120), 1:1.4 (S140), 1:1.6 (S160), 1:1.8 (S180), and 1:2.0 (S200). Second, by using Silicon Thinner as a softening agent, materials with low viscosity with intermediate compliance were attained as following ratios (EcoFlex 00-10 part A, part B, and Silicon Thinner, respectively): 1:0.8 (T80), 1:1.0 (T100), 1:1.2 (T120), 1:1.4 (T140), 1:1.6 (T160), 1:1.8 (T180), and 1:2.0 (T200). Since silicone-casted artificial skin of the robotic finger was made with the same base material without softening agents, soft objects used in the present experiment invariably had lower stiffness than that of the robotic skin of the finger.

The mixtures were poured in 3D-printed cylindrical molds with a diameter of 50 mm with a thickness of 40 mm. These objects are shown in the top panel of Fig. 3. Mechanical behavior of soft objects used in the present experiment is shown in Fig 3c. We picked one out of six pressure sensors embedded in the finger and analyzed the pressure response which corresponds to ramp and hold displacement inputs. The displacement of the object as acquired by the pressure sensor is plotted against time in Fig. 3c. From the figure, it can be seen that an observable difference in response was recorded with the objects with different degrees of viscosity.

C. Data Collection and Processing

To validate the proposed model, we collected data from 14 material specimens that we prepared in the previous step. The robotic finger presented in Sec. II-A was lowered onto each soft objects for 600 times. The indentation trajectory, i.e., displacement of the finger in normal to object surface direction h , was in the form of a half period of the sine wave $h = H * \sin(2\pi ft)$, where time varies $t \in (0, \frac{T}{2})$ with a step $dt = 1/125$, where T is the period. To vary the velocity of the indentation, the frequency of the wave f was randomly selected in a range 0.1 Hz and 1.5 Hz for each trial. Likewise, the indentation depth H was randomly sampled between 3 and 18 mm. The time between each indentation was set to 10 s, which was required for the shape recovery of the viscous samples. The posture of the finger relative to the soft object remained fixed throughout the experiment in such a way for all the six sensors to be in contact with the surface of the object in the manner shown in Fig. 2, except that the finger was displaced in normal to object surface direction.

The complete signals acquired from each soft object were normalized from zero to one by subtracting the minimum value of all signals and dividing by the maximum one. This is shown in Fig 4. This normalization strategy eliminated the possible bias, where magnitudes for harder samples are generally higher than the ones of the softer objects. The normalized signals, on other hand, preserved the spatial relation among pressure chambers, as well as temporal patterns. 500 randomly selected indentation time series were used for the training data set, whereas the remaining 100

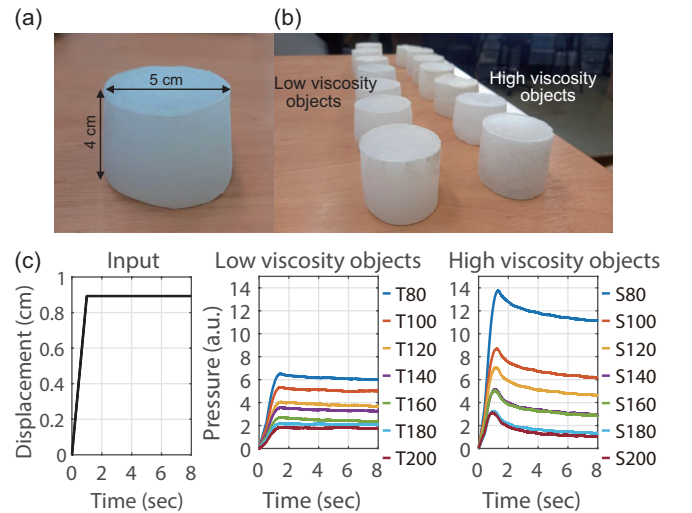


Fig. 3. (a) Low viscosity objects with varied compliance, and (b) high viscosity objects with varied compliance used in the experiments. Each sample has a weight of 72 g and approximate shape of a cylinder with a height of 4cm and a diameter of 5 cm. (c) The force response to ramp and hold displacement inputs, picked up by a single pressure sensor placed at the robotic finger. The overall magnitude of pressure and its decay rate are related to compliance and viscosity of the objects, respectively. Low viscosity objects were produced by mixing with Silicon Thinner as a softening agent, and high viscosity objects were produced by mixing Slacker as a softening agent. Signals were filtered to improve visibility. The prefixes S and T denotes objects with Slacker and Thinner, and the number denotes the percentage of softening agents relative to the amount of base materials.

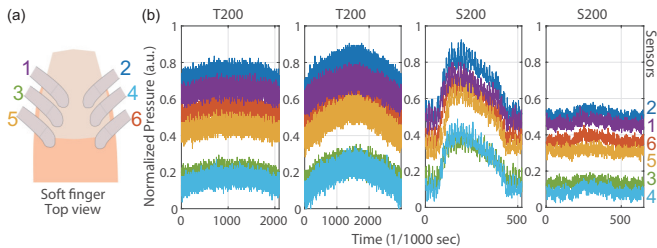


Fig. 4. (a) A top view of the soft finger with each pressure sensor numbered for clarity. (b) Examples of data from the pressure sensors connected to the six air chambers distributed at a tip of a soft anthropomorphic finger. Magnitudes of pressure from the sensors were normalized in the range 0 - 1. The amplitude of displacement and the frequency of indentation was randomized between 0.3 and 1.8 cm, and between 0.1 Hz and 1.5 Hz, respectively. The patterns of output from the six sensors varied depending on the amplitude and frequency of indentation, as well as the properties of the touched objects.

signals were for testing.

D. Softness Discrimination Model

The softness discrimination in our setup was defined in the form of classification. To capture both temporal and spatial features, we developed a neural network architecture based on Bi-directional Long Short-Time Memory (biLSTM) units. The LSTM belongs to a recurrent neural network (RNN) [26], which solves the vanishing gradient problem observed in classic RNN. The bi-directional version of LSTM, additionally to forward sequence, enables learning backward information at each step of a time [27].

The input of the proposed network was n -dimensional signal of arbitrary length, where n denotes the number of pressure sensors used for softness discrimination (see Fig. 5). The input layer was followed by the 100 biLSTM units. To prevent overfitting and ensure all biLSTM participates in learning, the drop-out layer was introduced before a fully-connected layer, which classifies the obtained spatiotemporal patterns into 14 classes. The probability of each class was obtained through exponential normalization by a softmax layer. To train the proposed network, we employed the Stochastic Gradient Descend (SGD) strategy with a minibatch size of 100. Weights of the network were updated using the Adaptive Moment Estimation (ADAM) optimizer with $1 - e3$ learning rate.

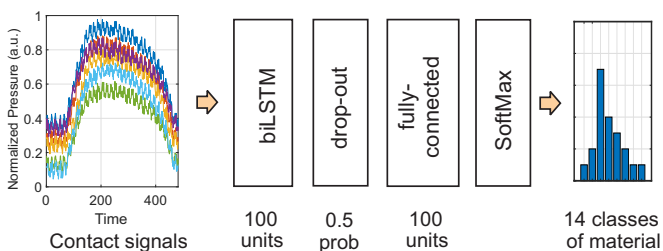


Fig. 5. Architecture of the biLSTM network used for learning of spatiotemporal features of the object softness.

E. Experiments

Based on the data set obtained from the interaction between soft robotic finger and fourteen material specimens that we prepared, the following three experiments were conducted to investigate the issue of how differences in available tactile information could impact the ability to distinguish the softness of viscoelastic materials with lower stiffness than that of a robotic skin.

1) *Experiment 1*: The LSTM network was trained for multi-class classification of fourteen soft objects that varied in compliance and viscosity, using the spatiotemporal patterns obtained from the six pressure sensors embedded in the soft robotic finger that interacted with the soft objects.

2) *Experiment 2*: To dissociate the effect of pressure distribution from that of local pressure dynamics, the LSTM network was trained for multiclass classification of soft objects using only the local pressure dynamics obtained from one of the six pressure sensors of the soft robotic finger.

3) *Experiment 3*: To investigate the effect of temporal structures such as hysteresis due to the viscosity of soft objects, the LSTM network was trained to discriminate soft objects using partial pressure time series obtained from interactions between the robotic finger and objects. The time series was split into two phases at the timing of maximum pressure as shown in Fig 9. The first half corresponded to the loading phase of the indentation event, and the second half corresponded to the relaxing phase, each of which was fed into the network separately for training.

III. RESULTS AND DISCUSSION

A. Experiment 1 - Tactile Discrimination Performance of Compliance by the Soft Robotic Finger

To test whether tactile information from six pressure sensors connected to air chambers embedded in the soft robotic finger can successfully discriminate the softness of objects without relying on the information about the displacement of the finger accompanying the indentation, we trained the LSTM network to discriminate the fourteen soft objects with different degrees of compliance and viscosity. The accuracy of the multi-class classification by the LSTM network reached 97.43%. The result strongly supported our hypothesis that the dynamics at the skin-object interface upon physical contact would provide sufficient information to distinguish the softness of soft viscoelastic objects (Fig. 6).

B. Experiment 2 - Effect of Spatial Distribution of Pressure

To further identify the nature of tactile information used, we compared the discrimination performance by the LSTM network between the condition where only local pressure information (i.e., the data from one pressure sensor on the finger) was available and the condition where the information about the spatial pattern of pressure (i.e., the data from six sensors distributed on the fingerpad) was also available. We hypothesized that the tactile information used by the finger to discriminate softness would be spatiotemporal in nature and that the discrimination performance would deteriorate when

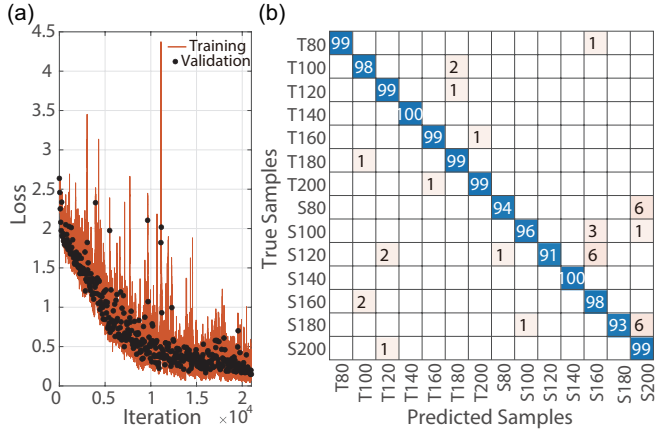


Fig. 6. (a) Training plot of the condition where data from the six sensors embedded in the soft finger was used. (b) Confusion matrix of the biLSTM network using six pressure sensors on the soft robotic finger trained for multi-class classification of fourteen soft objects. T80 to T200 represent soft objects with low viscosity made with Silicon Thinner as a softening agent. S80 to S200 represent soft objects with high viscosity made with Slacker as a softening agent. The number (e.g., S200) indicates the relative amount of softening agent in the object, where, as the number increases, the softness increases.

the information about the spatial distribution of pressure was not available.

Fig. 7 shows the accuracy of the multi-class discrimination under the conditions in which only the data from each of the six sensors was available, as well as the accuracy under the conditions in which the data from all sensors were available in combination. We observed that the accuracy of the multi-class discrimination decreased in the conditions where only local pressure information was available, confirming our second hypothesis. However, somewhat unexpectedly, even when the information about only local pressure and its change was available, the performance of multi-class classification of the fourteen objects still reached above 80% of accuracy. The opening question has to do with the nature of the information that local pressure changes could provide in discriminating soft objects with a moderate degree of accuracy.

As the experiments involved the seven soft objects with high viscosity made with Slacker as a softening agent (S80 to S200, the larger the number, the more compliant the object) and the seven soft objects with low viscosity made with Silicon Thinner as a softening agent (T80 to T200, the larger the number, the more compliant the object), we further looked into whether there is a difference in the accuracy of performance between the discrimination of objects with high viscosity and that of objects with low viscosity in the conditions where only one sensor was used to train the LSTM network. As can be seen in Fig. 8a, the LSTM network appeared to have performed better when discriminating objects with high viscosity compared to when discriminating the objects with low viscosity. When all the data from one-sensor trials were pooled (Fig. 8b), a paired t -test statistically confirmed that the accuracy of performance was indeed significantly higher for viscous objects compared to less-viscous counterparts, $t(41) = -5.84$, $p < 0.0001$. This

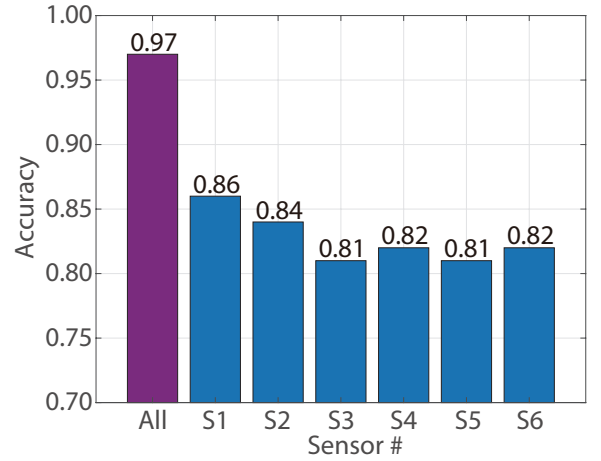


Fig. 7. Accuracy of discrimination of multi-class classification for fourteen soft objects in conditions where the different sensor was used.

result implies that complex local dynamics such as hysteresis in pressure changes arising from the viscosity of the material could have provided additional information that can be used in discriminating the viscoelasticity of soft objects, even when the information about pressure distribution over the contact region was unavailable.

C. Experiment 3 - Effect of Temporal Pressure Patterns

Given the different patterns in discrimination performance between objects with different degrees of viscosity in one-sensor conditions, we further looked into what aspect of the temporal characteristics in the indentation response of viscoelastic materials could provide information about the viscoelasticity of soft objects. We split the pressure time series into two phases at the peak of pressure as shown in Fig. 9, eliminating part of temporal information such as hysteresis

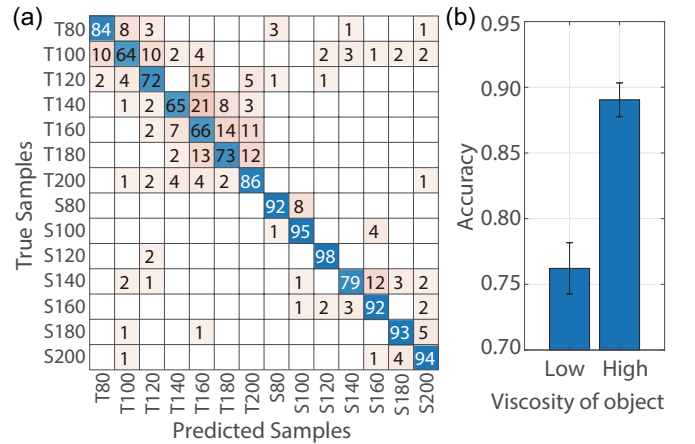


Fig. 8. (a) An example of a confusion matrix of the condition where data from only one sensor (sensor 3) was used to train the LSTM network for the multi-class classification of fourteen soft objects. (b) Accuracy of discrimination as a function of different types of soft objects (low viscosity vs. high viscosity objects) in the conditions where only one sensor on the fingertip was used (7 specimens by 6 sensor conditions yielded 42 accuracy values for each of the high and low viscosity objects). Error bars represent the standard error of means.

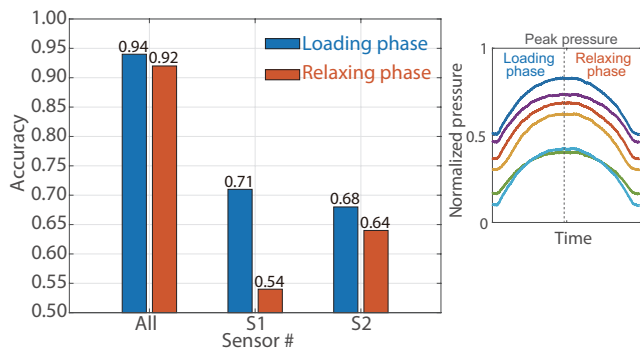


Fig. 9. Accuracy of discrimination of multi-class classification for fourteen soft objects in the two temporal phases of indentation (loading phase and relaxing phase) under different sensor conditions based on the data from all six sensors, and only sensor 1 or sensor 2 (the two best performing sensors in Experiment 2 where entire time series was used). The loading phase and relaxing phase were divided at the peak of the pressure time series. Pressure signals in the right panel were filtered to improve visibility.

response under dynamic loading and relaxing. Then we trained the LSTM network using each of the two halves of the pressure time series (i.e., loading phase and relaxing phase) for the multi-class classification of the fourteen soft objects.

This part of the experiment involved the conditions where the LSTM network was trained using each of the two sensors (sensors 1 and 2) that performed best in the previous discrimination task reported above (Fig 8), as well as the condition where the data from all the six sensors were available in combination. The results of the experiment are shown in Fig 9, which presents the accuracy of the prediction under the conditions in which different temporal phases of indentation were used (loading phase and relaxing phase), in different sensor conditions (six sensors, sensor 1 or 2 alone). Surprisingly, the accuracy of performance in the condition where the information about the distribution of pressure and its change was available (i.e., the condition where all the six sensors were used) was largely intact, attaining the discrimination accuracy above 90% in both loading and relaxing phase of the indentation, highlighting the robustness of information about softness available in the spatiotemporal structure of pressure distribution over the contact area.

By contrast, as expected, eliminating the part of temporal information resulted in a further decrease in discrimination accuracy in one-sensor conditions. The result suggests that the part of information about softness in local pressure dynamics was lost when the loading phase and relaxing phase were separated, implying the hysteresis response under dynamic loading and relaxing might have been among the discriminatory cues. We also observed that the accuracy was relatively high in the condition where pressure dynamics during the loading phase (i.e., the first half of the pressure time series) was available, compared to the conditions where pressure dynamics during the relaxing phase (the latter half of the pressure time series) was available. Given this result, it seems not improbable that there is certain information in the pattern of pressure change during the contact and loading

phase which the soft finger robot could take advantage of in discriminating soft viscoelastic materials.

IV. CONCLUSIONS

The development of technologies for sensing in soft robotics is a growing field with diverse potential solutions [1], [28]–[30]. The present study focused on the sensing softness of viscoelastic materials that had lower stiffness than that of soft robotic skin. We implemented human-inspired sensing of very soft objects in an anthropomorphic finger based on tactile information from complex dynamics at the skin-object interface, without using the information about indentation depth.

In the three experiments where LSTM networks were trained to discriminate fourteen viscoelastic soft objects, we demonstrated that the robotic finger could successfully learn to discriminate soft objects based on tactile information from six pressure sensors connected to the air chambers embedded in its soft skin. By dissociating the relative contribution of the dynamic pattern of pressure distribution and that of local pressure, we further demonstrated that the spatial distribution of pressure and its change over the contact region contained important information about the softness of touched objects. Additionally, we found that when only local pressure dynamics was used, the discrimination performance of the LSTM network was better for the objects with high viscosity compared to the objects with low viscosity. The result implied that nonlinear local dynamics such as hysteresis in pressure changes have provided additional information about viscoelasticity of the touched objects. These results highlighted how differences in available tactile information could impact the ability to distinguish soft viscoelastic materials that are ubiquitous in the natural environment.

ACKNOWLEDGMENT

This work was supported by the Engineering and Physical Sciences Research Council (EPSRC) RoboPatient grant EP/T00519X/1, by the SHERO project, a Horizon2020 Future and Emerging Technologies (FET) program of the European Commission (grant agreement ID 828818), by the European Union’s Horizon 2020 research and innovation programme under the Marie Skłodowska-Curie grant agreement No 101034337, and by the JSPS KAKENHI (grant numbers JP21H05823, JP21KK0182, JP22H00988). For the purpose of open access, the author has applied a Creative Commons Attribution (CC BY) licence to any Author Accepted Manuscript version arising.

REFERENCES

- [1] T. G. Thuruthel, B. Shih, C. Laschi, and M. T. Tolley, “Soft robot perception using embedded soft sensors and recurrent neural networks,” *Science Robotics*, vol. 4, no. 26, p. eaav1488, 2019.
- [2] N. R. Sinatra, C. B. Teeple, D. M. Vogt, K. K. Parker, D. F. Gruber, and R. J. Wood, “Ultragentle manipulation of delicate structures using a soft robotic gripper,” *Science Robotics*, vol. 4, no. 33, p. eaax5425, 2019.

- [3] O. A. Araromi, M. A. Graule, K. L. Dorsey, S. Castellanos, J. R. Foster, W.-H. Hsu, A. E. Passy, J. J. Vlassak, J. C. Weaver, C. J. Walsh, *et al.*, “Ultra-sensitive and resilient compliant strain gauges for soft machines,” *Nature*, vol. 587, no. 7833, pp. 219–224, 2020.
- [4] P. Hyatt, D. Kraus, V. Sherrod, L. Rupert, N. Day, and M. D. Killpack, “Configuration estimation for accurate position control of large-scale soft robots,” *IEEE/ASME Transactions on Mechatronics*, vol. 24, no. 1, pp. 88–99, 2018.
- [5] L. O. Tiziani and F. L. Hammond, “Optical sensor-embedded pneumatic artificial muscle for position and force estimation,” *Soft robotics*, vol. 7, no. 4, pp. 462–477, 2020.
- [6] J. Zhu, A. Cherubini, C. Dune, D. Navarro-Alarcon, F. Alambeigi, D. Berenson, F. Ficuciello, K. Harada, J. Kober, X. Li, *et al.*, “Challenges and outlook in robotic manipulation of deformable objects,” *IEEE Robotics & Automation Magazine*, vol. 29, no. 3, pp. 67–77, 2022.
- [7] X. Ma, Y. Ye, H. Meng, W. Wang, W. Wang, and G. Bao, “Sensor embedded soft fingertip for precise manipulation and softness recognition,” *IEEE Robotics and Automation Letters*, vol. 6, no. 4, pp. 8734–8741, 2021.
- [8] Z. Cui, W. Wang, L. Guo, Z. Liu, P. Cai, Y. Cui, T. Wang, C. Wang, M. Zhu, Y. Zhou, *et al.*, “Haptically quantifying young’s modulus of soft materials using a self-locked stretchable strain sensor,” *Advanced Materials*, vol. 34, no. 25, p. 2104078, 2022.
- [9] M. Di Luca, *Multisensory softness*. Springer, 2014.
- [10] W. M. B. Tiest and A. M. Kappers, “Cues for haptic perception of compliance,” *IEEE transactions on haptics*, vol. 2, no. 4, pp. 189–199, 2009.
- [11] C. Xu, Y. Wang, S. C. Hauser, and G. J. Gerling, “In the tactile discrimination of compliance, perceptual cues in addition to contact area are required,” in *Proceedings of the Human Factors and Ergonomics Society Annual Meeting*, vol. 62, no. 1. SAGE Publications Sage CA: Los Angeles, CA, 2018, pp. 1535–1539.
- [12] Y. Visell and S. Okamoto, “Vibrotactile sensation and softness perception,” in *Multisensory softness*. Springer, 2014, pp. 31–47.
- [13] M. A. Srinivasan and R. H. LaMotte, “Tactual discrimination of softness,” *Journal of neurophysiology*, vol. 73, no. 1, pp. 88–101, 1995.
- [14] C. Dhong, R. Miller, N. B. Root, S. Gupta, L. V. Kayser, C. W. Carpenter, K. J. Loh, V. S. Ramachandran, and D. J. Lipomi, “Role of indentation depth and contact area on human perception of softness for haptic interfaces,” *Science advances*, vol. 5, no. 8, p. eaaw8845, 2019.
- [15] A. Bicchi, E. P. Scilingo, and D. De Rossi, “Haptic discrimination of softness in teleoperation: the role of the contact area spread rate,” *IEEE Transactions on Robotics and Automation*, vol. 16, no. 5, pp. 496–504, 2000.
- [16] W. M. Bergmann Tiest and A. M. Kappers, “Physical aspects of softness perception,” in *Multisensory softness*. Springer, 2014, pp. 3–15.
- [17] B. Li and G. J. Gerling, “Individual differences impacting skin deformation and tactile discrimination with compliant elastic surfaces,” in *2021 IEEE World Haptics Conference (WHC)*. IEEE, 2021, pp. 721–726.
- [18] C. Xu, Y. Wang, and G. J. Gerling, “Individual performance in compliance discrimination is constrained by skin mechanics but improved under active control,” in *2021 IEEE World Haptics Conference (WHC)*. IEEE, 2021, pp. 445–450.
- [19] —, “An elasticity-curvature illusion decouples cutaneous and proprioceptive cues in active exploration of soft objects,” *PLoS computational biology*, vol. 17, no. 3, p. e1008848, 2021.
- [20] M. Cavdan, K. Doerschner, and K. Drewing, “Haptic discrimination of different types of soft materials,” in *International Conference on Human Haptic Sensing and Touch Enabled Computer Applications*. Springer, 2022, pp. 3–11.
- [21] O. Caldiran, H. Z. Tan, and C. Basdogan, “Visuo-haptic discrimination of viscoelastic materials,” *IEEE Transactions on Haptics*, vol. 12, no. 4, pp. 438–450, 2019.
- [22] S.-J. Estermann, D. H. Pahr, and A. Reisinger, “Material design of soft biological tissue replicas using viscoelastic micromechanical modelling,” *Journal of the Mechanical Behavior of Biomedical Materials*, vol. 125, p. 104875, 2022.
- [23] K. Gilday, L. Relandeau, and F. Iida, “Design and characterisation of a soft barometric sensing skin for robotic manipulation,” in *2022 IEEE/RSJ International Conference on Intelligent Robots and Systems (IROS 2022)*. IEEE, 2022.
- [24] H. Wang, T. G. Thuruthel, K. Gilday, A. Abdulali, and F. Iida, “Machine learning for soft robot sensing and control: A tutorial study,” in *2022 IEEE 5th International Conference on Industrial Cyber-Physical Systems (ICPS)*. IEEE, 2022, pp. 01–06.
- [25] A. Dargahi, R. Sedaghati, and S. Rakheja, “On the properties of magnetorheological elastomers in shear mode: Design, fabrication and characterization,” *Composites Part B: Engineering*, vol. 159, pp. 269–283, 2019.
- [26] S. Hochreiter and J. Schmidhuber, “Long short-term memory,” *Neural computation*, vol. 9, no. 8, pp. 1735–1780, 1997.
- [27] A. Graves and J. Schmidhuber, “Framewise phoneme classification with bidirectional lstm and other neural network architectures,” *Neural networks*, vol. 18, no. 5-6, pp. 602–610, 2005.
- [28] B. Shih, D. Shah, J. Li, T. G. Thuruthel, Y.-L. Park, F. Iida, Z. Bao, R. Kramer-Bottiglio, and M. T. Tolley, “Electronic skins and machine learning for intelligent soft robots,” *Science Robotics*, vol. 5, no. 41, p. eaaz9239, 2020.
- [29] T. G. Thuruthel, J. Hughes, A. Georgopoulou, F. Clemens, and F. Iida, “Using redundant and disjoint time-variant soft robotic sensors for accurate static state estimation,” *IEEE Robotics and Automation Letters*, vol. 6, no. 2, pp. 2099–2105, 2021.
- [30] K. Gilday, J. Hughes, and F. Iida, “Sensing, actuating, and interacting through passive body dynamics: A framework for soft robotic hand design,” *Soft Robotics*, vol. 10, no. 1, pp. 159–173, 2023.